New 3d–4f Heterometallic Coordination Polymers Based on Pyrazole-Bridged Cu II Ln III Dinuclear Units and Sulfate Anions: Syntheses, Structures, and Magnetic Properties

ARTICLE *in* CRYSTAL GROWTH & DESIGN · FEBRUARY 2009

Impact Factor: 4.89 · DOI: 10.1021/cg800848n

Article

New 3d#4f Heterometallic Coordination Polymers Based on Pyrazole-Bridged CuLn Dinuclear Units and Sulfate Anions: Syntheses, Structures, and Magnetic Properties

Xin-Hui Zhou, Yan-Hong Peng, Xiao-Di Du, Cai-Feng Wang, Jing-Lin Zuo, and Xiao-Zeng You

Cryst. Growth Des., **2009**, 9 (2), 1028-1035• DOI: 10.1021/cg800848n • Publication Date (Web): 19 December 2008

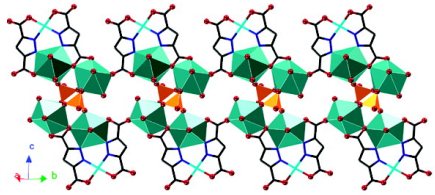

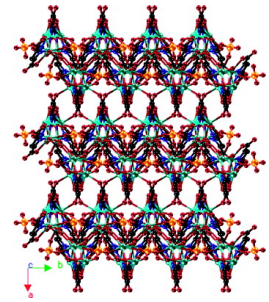

CRYSTAL GROWTH & DESIGN
2009
VOL. 9, NO. 2
1028–1035

New 3d−4f Heterometallic Coordination Polymers Based on Pyrazole-Bridged $Cu^{II}Ln^{III}$ Dinuclear Units and Sulfate Anions: Syntheses, Structures, and Magnetic Properties

Xin-Hui Zhou, Yan-Hong Peng, Xiao-Di Du, Cai-Feng Wang, Jing-Lin Zuo,* and Xiao-Zeng You

State Key Laboratory of Coordination Chemistry, Nanjing National Laboratory of Microstructures, School of Chemistry and Chemical Engineering, Nanjing University, Nanjing 210093, People's Republic of China

Received August 3, 2008; Revised Manuscript Received October 24, 2008

ABSTRACT: A series of 3d−4f heterometallic coordination polymers $\{[CuLn_2(pdc)_2(SO_4)(H_2O)_6]\cdot H_2O\}_n$ (Ln = Tb (**1**), Dy (**2**); H_3pdc = 3,5-pyrazoledicarboxylic acid), $\{[CuLn_2(pdc)_2(SO_4)(H_2O)_4]\cdot H_2O\}_n$ (Ln = Sm (**3**), Eu (**4**), Gd (**5**), Tb (**6**), Dy (**7**)) have been hydrothermally synthesized and structurally characterized. The sulfate anions were in situ obtained from oxidation of CuSCN during the reaction. Complexes **1**−**7** are all constructed from pyrazole-bridged $Cu^{II}Ln^{III}$ dinuclear units and sulfate anions. Complexes **1** and **2** are isostructural and possess an infinite double-stranded tapelike 1D coordination framework. However, complexes **3**−**7** are interesting 3d−4f heterometallic coordination polymers with similar 3D framework structures. The magnetic properties of compounds **2**, **4**−**6** have been investigated through the magnetic measurements over the temperature range of 1.8−300 K.

Introduction

The design and construction of lanthanide mixed-transition-metal (3d−4f) heterometallic complexes is important in coordination chemistry because of their structural and topological diversity and their potential applications in catalysis, electronic apparatus, magnetic materials, molecular sensors, etc.[1,2] In literatures, a large number of complexes containing both lanthanide and transition metal ions have been reported. However, the understanding of the magnetic exchange interactions between rare-earth and transition-metal ions is less advanced, because most Ln^{III} ions have an orbital contribution.[3] Compared to the work on 3d−4f systems with magnetic bridges such as cyanide, carbonyl, carboxyl and hydroxyl,[4] the use of pyrazole ligand to construct 3d−4f complexes for magnetic studies is less developed so far.[5]

Anions play an important role in the structural control for self-assembly.[6] The most common anions known to be employed in organic−inorganic are silicates,[7] phosphates[8] and carboxylates.[9] Sulfate ions have the versatile coordination modes and can lead to a diversity of frameworks in conjunction with the flexibility coordination of the lanthanide ions.[10] However, open-framework structure based upon lanthanide sulfates has been less documented.

The multifunctional ligand, 3,5-pyrazoledicarboxylic acid (H_3pdc) (Scheme 1), has multiple coordination sites involving two pyrazole nitrogen atoms and four carboxylate oxygen atoms. It has three different abstractable hydrogens and is good for constructing pyrazole-bridged heterometallic complexes.[11] The planar and heteroaromatic dicarboxylates are sterically compact and allow metal−metal interactions through π orbitals. Moreover, it can hold metal ions even closer compared with other five-membered diaza ring systems.[12] Based on this versatile ligand, although lots of complexes with transition-metal or lanthanide ions have been reported,[11,12] 3d−4f heterometallic complex is rarely reported before.

Herein, we report the syntheses, crystal structures and magnetic properties of seven heterometallic 3d−4f complexes

Scheme 1

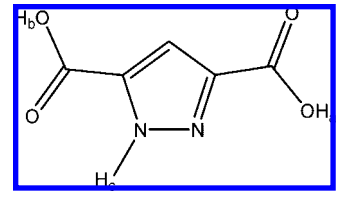

obtained by hydrothermal reactions of $Ln(NO_3)_3\bullet nH_2O$, CuSCN and H_3pdc in water: $\{[CuTb_2(pdc)_2(SO_4)(H_2O)_6]\bullet H_2O\}_n$ (**1**), $\{[CuDy_2(pdc)_2(SO_4)(H_2O)_6]\bullet H_2O\}_n$ (**2**), $\{[CuSm_2(pdc)_2(SO_4)(H_2O)_4]\bullet H_2O\}_n$ (**3**), $\{[CuEu_2(pdc)_2(SO_4)(H_2O)_4]\bullet H_2O\}_n$ (**4**), $\{[CuGd_2(pdc)_2(SO_4)(H_2O)_4]\bullet H_2O\}_n$ (**5**), $\{[CuTb_2(pdc)_2(SO_4)(H_2O)_4]\bullet H_2O\}_n$ (**6**) and $\{[CuDy_2(pdc)_2(SO_4)(H_2O)_4]\bullet H_2O\}_n$ (**7**). They all consist of the pyrazole-bridged $Cu^{II}Ln^{III}$ dinuclear units and sulfate anions.

Experimental Section

Synthesis. The lanthanide(III) nitrates were converted from their oxides by nitric acid. Other reagents and solvents were purchased from commercial sources and used as received. Elemental analyses for C, H, and N were performed on a Perkin-Elmer 240C analyzer. Infrared spectra were recorded on a Vector22 Bruker Spectrophotometer with KBr pellets in the 400−4000 cm^{-1} region. Magnetic susceptibility measurements of polycrystalline samples were measured over the temperature range 1.8−300 K with a Quantum Design MPMS-XL7 SQUID magnetometer.

Syntheses of 1−7. A mixture of H_3pdc, $Ln(NO_3)_3\cdot nH_2O$ and CuSCN in the ratio of 2:2:1 was added to 10 mL of the deionized water. After the mixture was stirred for 30 min (solution pH 5), it was placed in a 25 mL Teflon-lined reactor and heated at 180 °C in an oven for 2 days and then slowly cooled to room temperature. Block crystals of **1**−**7** suitable for X-ray diffraction analysis were isolated (yield ca. 23% for **1**, 54% for **2**, 18% for **3**, 45% for **4**, 57% for **5**, 48% for **6**, and 15% for **7** based on $Ln(NO_3)_3$). Anal. Calcd for **1**: C, 13.20; H, 1.77; N, 6.16. Found: C, 13.01; H, 1.68; N, 6.02%. For **2**: C, 13.10; H, 1.76; N, 6.11. Found: C, 12.92; H, 1.64; N, 5.98%. For **3**: C, 14.02; H, 1.41; N, 6.54. Found: C, 13.85; H, 1.30; N, 6.42%. For **4**: C, 13.97; H, 1.41; N, 6.52. Found: C, 13.87; H, 1.34; N, 6.45%. For **5**: C, 13.80; H, 1.39; N, 6.44. Found: C, 13.65; H, 1.32; N, 6.37%. For **6**: C, 13.75; H, 1.38; N, 6.41. Found: C, 13.67; H, 1.31; N, 6.32%. For **7**: C, 13.64; H, 1.37; N,

* To whom correspondence should be addressed. E-mail: zuojl@nju.edu.cn. Fax: 86-25-83314502.

10.1021/cg800848n CCC: $40.75
Published on Web 12/19/2008

Table 1. Crystallographic Data for Complexes 1−7

	1	**2**	**3**	**4**	**5**	**6**	**7**
formula	$C_{10}H_{16}CuN_4O_{19}STb_2$	$C_{10}H_{16}CuN_4O_{19}SDy_2$	$C_{10}H_{12}CuN_4O_{17}SSm_2$	$C_{10}H_{12}CuN_4O_{17}SEu_2$	$C_{10}H_{12}CuN_4O_{17}SGd_2$	$C_{10}H_{12}CuN_4O_{17}STb_2$	$C_{10}H_{12}CuN_4O_{17}SDy_2$
fw	909.71	916.87	856.54	859.76	870.34	873.68	880.84
cryst syst	triclinic	triclinic	monoclinic	monoclinic	monoclinic	monoclinic	monoclinic
space group	$P\bar{1}$	$P\bar{1}$	$P2(1)/c$	$P2(1)/c$	$P2(1)/c$	$P2(1)/c$	$P2(1)/c$
a (Å)	7.132(1)	7.1295(9)	12.277(2)	12.270(1)	12.266(2)	12.212(4)	12.202(2)
b (Å)	10.257(2)	10.251(1)	6.894(1)	6.8833(7)	6.863(1)	6.814(2)	6.780(1)
c (Å)	15.589(3)	15.583(2)	23.769(4)	23.757(2)	23.739(3)	23.693(7)	23.664(4)
α (deg)	80.826(3)	80.709(2)	90.00	90.00	90.00	90.00	90.00
β (deg)	79.755(3)	79.568(2)	95.294(3)	95.216(2)	95.118(3)	95.087(6)	94.750(2)
γ (deg)	76.877(3)	76.666(2)	90.00	90.00	90.00	90.00	90.00
V (Å^3)	1084.5(3)	1081.3(2)	2003.2(5)	1998.1(3)	1990.6(5)	1963.8(10)	1951.1(5)
Z	2	2	4	4	4	4	4
D_{calcd} (g cm^{-3})	2.786	2.816	2.840	2.858	2.904	2.955	2.999
T(K)	293(2)	293(2)	293(2)	293(2)	293(2)	293(2)	293(2)
μ (mm^{-1})	7.622	8.015	7.042	7.460	7.850	8.405	8.870
F(000)	862	866	1620	7.460	1636	1644	1652
no. of reflns collected	5802	5777	9580	9402	9512	9353	9232
unique reflections	4130	4120	3521	3517	3495	3459	3423
GOF (F^2)	1.053	1.122	1.163	1.132	1.092	0.883	1.092
R_1,[a] wR_2[b] ($I > 2\sigma(I)$)	0.0409, 0.1073	0.0357, 0.0988	0.0540, 0.0980	0.0370, 0.0820	0.0389, 0.0844	0.0433, 0.0700	0.0495, 0.1295
R_1,[a] wR_2[b] (all data)	0.0441, 0.1096	0.0375, 0.1002	0.0676, 0.1021	0.0408, 0.0839	0.0455, 0.0870	0.0610, 0.0748	0.0521, 0.1321

[a] $R_1 = \sum||F_o| - |F_c||/\sum F_o|$. [b] $wR_2 = [\sum w(F_o^2 - F_c^2)^2/\sum w(F_o^2)]^{1/2}$.

6.36. Found: C, 13.52; H, 1.28; N, 6.26%. IR (KBr)/cm^{-1} for **1**: 3172 s, 1578 vs, 1505 s, 1451 w, 1398 m, 1136 s, 1067 w, 1010 w, 695 w, 623 w. For **2**: 3171 s, 1580 s, 1506 m, 1450 w, 1392 m, 1137 m, 1066 w, 1012 w, 694 w, 625 w. For **3**: 3140 s, 1657 s, 1623 s, 1527 m, 1508 m, 1398 m, 1134 s, 1066 m, 1014 w, 643 w, 620 w. For **4**: 3139 m, 1656 s, 1624 s, 1526 m, 1506 s, 1397 m, 1135 s, 1065 m, 1015 w, 644 w, 621 m. For **5**: 3140 m, 1654 s, 1624 vs, 1529 m, 1507 s, 1399 m, 1133 s, 1066 m, 1016 m, 644 w, 622 w. For **6**: 3140 m, 1658 s, 1624 s, 1531 s, 1508 s, 1400 m, 1133 s, 1066 s, 1016 m, 644 w, 622 m. For **7**: 3137 s, 1660 m, 1623 s, 1530 s, 1509 s, 1401 m, 1132 s, 1068 s, 1014 m, 647 w, 620 w.

X-ray Crystallography. The crystal structures of complexes **1**−**7** were determined on a Siemens (Bruker) SMART CCD diffractometer using monochromated Mo-$K\alpha$ radiation (λ = 0.71073 Å) at room temperature. Cell parameters were retrieved using SMART software and refined using SAINT[13] on all observed reflections. Data were collected using a narrow-frame method with scan widths of 0.30° in ω and an exposure time of 10 s/frame. The highly redundant data sets were reduced using SAINT[13] and corrected for Lorentz and polarization effects. Absorption corrections were applied using SADABS[14] supplied by Bruker. Structures were solved by direct methods using the program SHELXL-97.[15] The positions of the metal atoms and their first coordination spheres were located from direct-method E maps; other non-hydrogen atoms were found using alternating difference Fourier syntheses and least-squared refinement cycles and, during the final cycles, were refined anisotropically. Hydrogen atoms were placed in calculated position and refined as riding atoms with a uniform value of U_{iso}. Crystallographic details have been summarized in Table 1. Selected bond lengths for **2** and **5** were given in Table 2. Selected bond lengths for **1**, **3**, **4**, **6**, and **7** were given in the Supporting Information.

Table 2. Selected Bond Lengths (Å) for Complexes 2[a] and 5[b]

	Complex **2**		
Cu(1)−N(2)	1.924(5)	Cu(1)−N(3)	1.902(5)
Cu(1)−O(4)	1.969(4)	Cu(1)−O(5)	1.973(4)
Dy(1)−N(1)	2.458(5)	Dy(1)−N(4)	2.499(5)
Dy(1)−O(2)	2.353(4)	Dy(1)−O(8)	2.359(4)
Dy(1)−O(9)	2.335(5)	Dy(1)−O(10)	2.351(5)
Dy(1)−O(11)	2.484(4)	Dy(1)−O(12)	2.344(4)
Dy(2)−O(1a)	2.376(5)	Dy(2)−O(7)	2.361(5)
Dy(2)−O(8)	2.528(4)	Dy(2)−O(13b)	2.332(4)
Dy(2)−O(15)	2.433(5)	Dy(2)−O(16)	2.378(5)
Dy(2)−O(17)	2.344(5)	Dy(2)−O(18)	2.322(5)
	Complex **5**		
Cu(1)−N(2)	1.925(6)	Cu(1)−N(3)	1.902(7)
Cu(1)−O(4)	1.991(6)	Cu(1)−O(5)	1.989(6)
Cu(1)−O(9)	2.364(7)	Gd(1)−N(1)	2.540(6)
Gd(1)−N(4)	2.531(6)	Gd(1)−O(2)	2.588(5)
Gd(1)−O(2d)	2.446(5)	Gd(1)−O(8)	2.497(5)
Gd(1)−O(10)	2.709(6)	Gd(1)−O(11)	2.384(5)
Gd(1)−O(13b)	2.391(6)	Gd(1)−O(14d)	2.369(6)
Gd(2)−O(1d)	2.325(6)	Gd(2)−O(3a)	2.772(5)
Gd(2)−O(4a)	2.422(5)	Gd(2)−O(6c)	2.375(6)
Gd(2)−O(7)	2.449(5)	Gd(2)−O(8)	2.530(5)
Gd(2)−O(15)	2.471(6)	Gd(2)−O(12b)	2.320(5)
Gd(2)−O(16)	2.458(6)		

[a] Symmetry transformation codes: a $1 + x, -1 + y, z$; b $1 - x, -y, 1 - z$; [b] Symmetry transformation codes: a $x, 1.5 - y, 0.5 + z$; b $x, 1 + y, z$; c $2 - x, 2 - y, 2 - z$; d $1 - x, 1 - y, 2 - z$; e $x, 1.5 - y, -0.5 + z$; f $x, -1 + y, z$.

Results and Discussion

Preparations of 1−7. Complexes **1**−**7** were obtained by the hydrothermal reactions of H_3pdc, $Ln(NO_3)_3 \cdot nH_2O$ and CuSCN in water. The sulfate anions were in situ obtained by oxidation of CuSCN from dilute HNO_3 during the reaction. Although the starting materials are copper(I) salts, the Cu centers in **1**−**7** have an oxidation state of +2, resulted from the oxidation reaction of CuSCN. Importantly, if CuSCN was replaced by CuX (X = Cl, Br, I, CN) and the sulfate anions were introduced directly into the reaction, no similar target products were observed after the workup of the reactions.**1** and **6**, **2** and **7** are synthesized in one-pot reaction, respectively.

Infrared spectra of **1**−**7** show characteristic bands in the region from 1160 to 1000 cm^{-1} due to ν_1 and ν_3 of the sulfate groups.[16] All carboxyl groups of H_3pdc ligand in complexes **1**−**7** are deprotonated, in agreement with the IR data in which no strong absorption peaks ranging from 1690 to 1730 cm^{-1} for −COOH are observed. The strong peaks are around 1580−1400 cm^{-1} for **1** and **2** and 1660−1400 cm^{-1} for **3**−**7**, which is characteristic of the expected absorption for asymmetric and symmetric vibrations of the carboxylate groups.

Structures of 1 and 2. Single-crystal X-ray analysis reveals that complexes **1** and **2** crystallize in the triclinic space group $P\bar{1}$ and comprise an infinite double-stranded tapelike 1D coordination framework. Since they are isostructural, only the structure of **2** is described here in detail (Figure 1). The asymmetric unit of **2** contains two crystallographically independent dysprosium ions, one copper ion, two pdc^{3-} ligands with two different coordination modes (Scheme 2), one sulfate anion, six coordinated water molecules, and one solvated water molecule. Each Cu^{2+} ion is four-coordinated and chelated by two pdc^{3-} through two carboxylate oxygen atoms (O(4) and O(5)) and two pyrazole nitrogen atoms (N(2) and N(3)). The

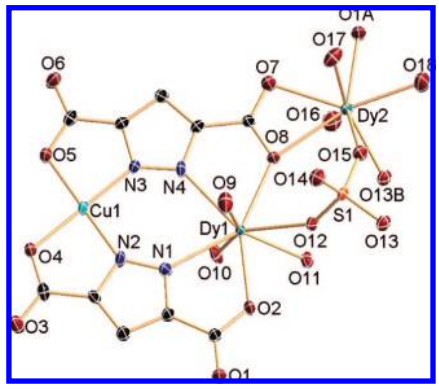

Figure 1. Coordination environments of Dy and Cu atoms in **2** with the thermal ellipsoids drawn at the 50% probability level. All H atoms and noncoordinated water molecules are omitted for clarity. Symmetry codes for the generated atoms see Table 2.

coordination geometry around Cu^{2+} ion is slightly distorted square-planar. The Cu−O bond lengths range from 1.969(4) to 1.973(4) Å and the Cu−N bond lengths range from 1.902(5) to 1.924(5) Å (Table 2). The Dy(1) center is also chelated by two pdc^{3-} and the two pdc^{3-} simultaneously connect the Cu(1) center as the bridges, leading to the formation of an interesting pyrazole-bridged heterometallic $Cu^{II}Dy^{III}$ dinuclear unit. In this dinuclear unit, the distance between Cu(1) and Dy(1) is 4.544 Å and the dihedral angle between two pyrazole rings is 1.8°. All the atoms of the $Cu^{II}Dy^{III}$ dinuclear unit lie in an approximate plane with the largest deviation of 0.1788 Å (Dy(1) atom from the mean plane defined by the two pyrazole rings). The Dy(1) and Dy(2) centers are both eight-coordinated and have distorted bicapped trigonal prismatic coordination environments: one sulfate oxygen atom (O(12)), three water molecules (O(9), O(10) and O(11)), two carboxylate oxygen atoms (O(2) and O(8)), and two pyrazole nitrogen atoms (N(1) and N(4)) from two pdc^{3-} ligands for Dy(1); two sulfate oxygen atoms (O(13b) and O(15)), three carboxylate oxygen atoms (O(1a), O(7) and O(8)) from two pdc^{3-} ligands, and three water molecules (O(16), O(17) and O(18)) for Dy(2). The Dy−O bond lengths range from 2.335(5) to 2.528(4) Å and the Dy−N bond lengths range from 2.458(5) to 2.499(5) Å (Table 2).

The two pdc^{3-} ligands in the asymmetric unit of **2** adopt two coordination modes (a and b) as depicted in Scheme 2. In coordination mode a, the pdc^{3-} ligand acts in a μ_6-η^2N,O,η^2N′,O′,η^2O′,O″ fashion, chelating the Cu(1), Dy(1) and Dy(2) centers, respectively. In mode b, the pdc^{3-} ligand binds in a μ_5-η^2N,O,η^2N′,O″,η^1O‴ fashion, chelating the Cu(1) and Dy(1) centers and bridging the Dy(2) center, respectively. The sulfate anions are tridentate (Scheme 2e) and bridge to three Dy(III) ions (Dy(1), Dy(2), and Dy(2b)).

The Dy(1) and Dy(2) centers are alternatively bridged by the anti−anti carboxylate group of pdc^{3-} and μ_2-O(8) to form an infinite 1D chain (Figure 2a), in which the distances between Dy(1) and Dy(2) centers are 4.691 and 6.826 Å, respectively. Two chains are connected together by the μ_3-SO_4^{2-} bridges to construct an infinite double-stranded tapelike 1D coordination framework (Figure 2c), where an eight-membered ring $Dy_2S_2O_4$ is formed (Figure 2b). As shown in Figure 2d, the $Cu^{II}Dy^{III}$ dinuclear units are almost coplanar in double-stranded 1D chains.

Structures of 3−7. Complexes **3**−**7** are isostructural: all crystallize in the monoclinic space group $P2_1/c$ and possess novel 3d−4f heterometallic coordination polymers with an interesting 3D framework structure. The structure of complex **5** is described in detail (Figure 3). The asymmetric unit contains two crystallographically independent gadolinium ions, one copper ion, two pdc^{3-} ligands with two different coordination modes (Scheme 2), one sulfate anion, four coordinated water molecules, and one solvated water molecule. Each Cu^{2+} ion is five-coordinated by one water molecule (O(9)), two carboxylate oxygen atoms (O(4) and O(5)), and two pyrazole nitrogen atoms (N(2) and N(3)) from two pdc^{3-} ligands. The coordination geometry around Cu^{2+} ion is a slightly distorted square-pyramid. The Cu−O(COO$^-$) bond lengths range from 1.989(6) to 1.991(6) Å, the Cu−O(H_2O) bond length is 2.364(7) Å and the Cu−N bond lengths range from 1.902(7) to 1.925(6) Å (Table 2). Two pdc^{3-} ligands and the Cu(1) and Gd(1) centers in the asymmetric unit also give an interesting pyrazole-bridged heterometallic $Cu^{II}Gd^{III}$ dinuclear unit. In each dinuclear unit, the distance between Cu(1) and Gd(1) is 4.474 Å, although the dihedral angle between two pyrazole rings is 27.0°, which is much bigger than that for **2**. So the two pdc^{3-} ligands are folded to form a sawhorse type structure. The Gd(1) and Gd(2) centers are both nine-coordinated and have distorted tricapped trigonal prismatic coordination environments: three sulfate oxygen atoms (O(11), O(13b), and O(14d)), one water molecule (O(10)), three carboxylate oxygen atoms (O(2), O(2d), and O(8)), and two pyrazole nitrogen atoms (N(1)and N(4)) from the pdc^{3-} ligands for Gd(1); one sulfate oxygen atom (O(12b)), six carboxylate

Scheme 2. Coordination Modes of the Ligand pdc^{3-} and SO_4^{2-} Ion in 1 and 2 (a, b, e) and in 3−7 (c, d, f)

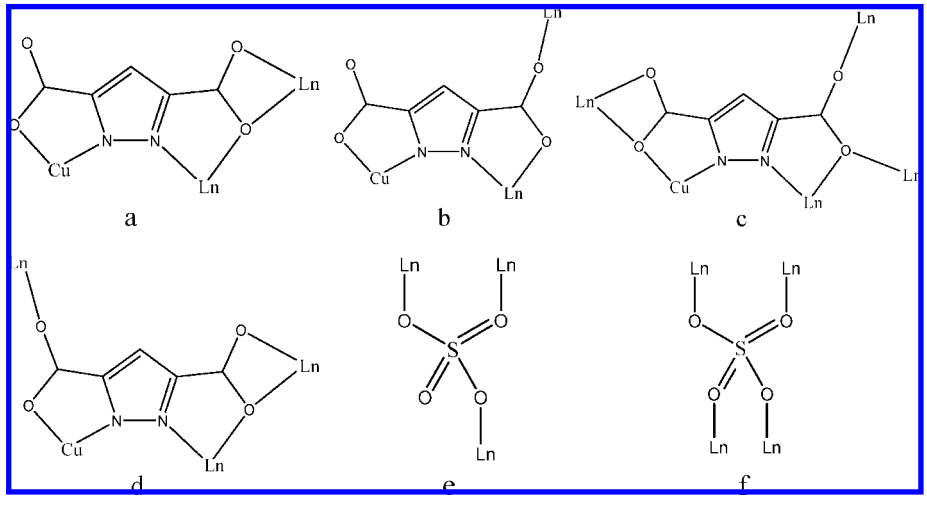

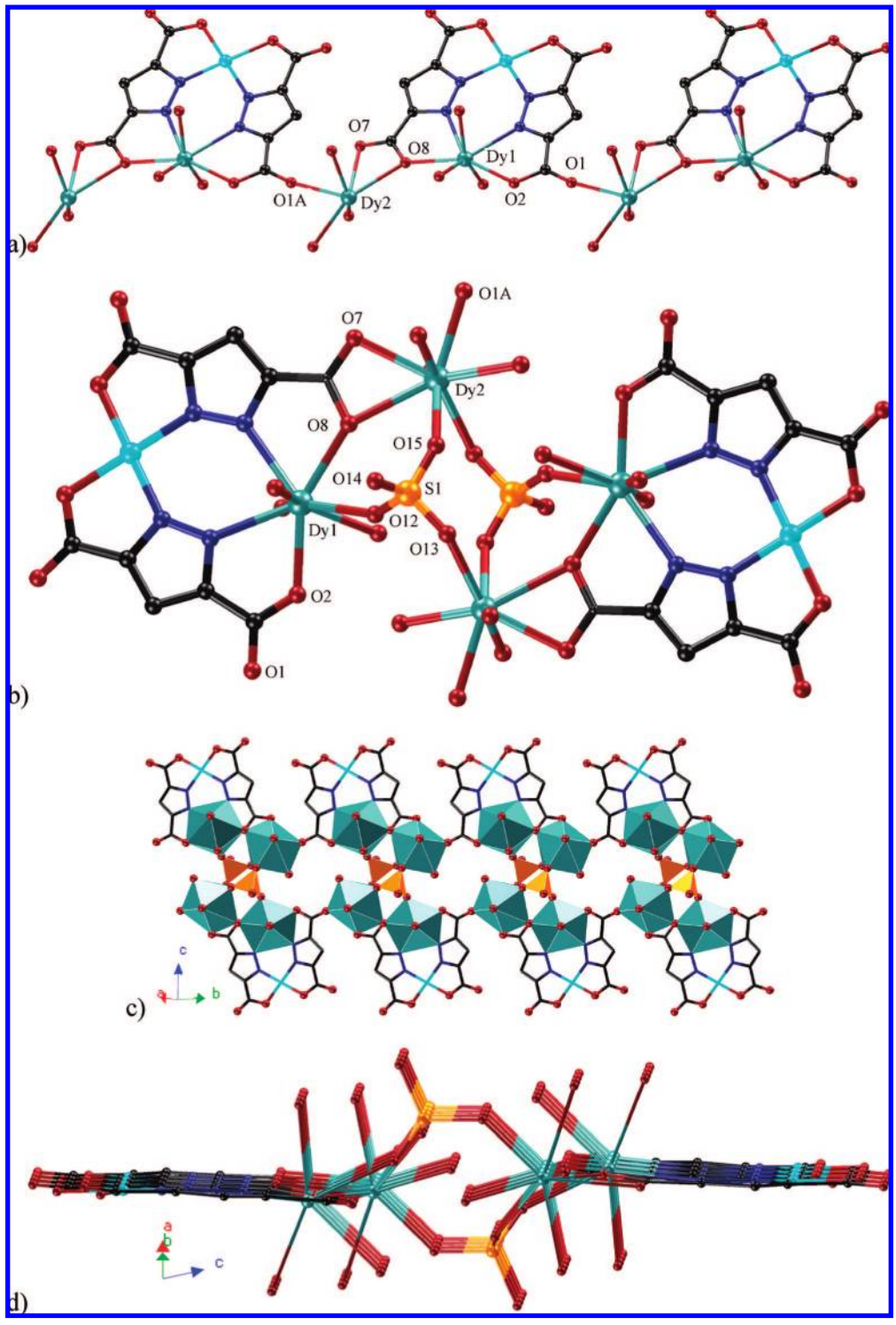

Figure 2. (a) Connections between Dy1 and Dy2 through carboxylate oxygen. (b) Coordination environments of SO_4^{2-} in **2**. The double-stranded tapelike 1D chain of **2** viewed along two different directions (c) and (d).

oxygen atoms (O(1d), O(3a), O(4a), O(6c), O(7), and O(8)) from four pdc^{3-} ligands, and two water molecules (O(15) and O(16)) for Gd(2). The Gd−O bond lengths range from 2.320(5) to 2.772(5) Å and the Gd−N bond lengths range from 2.531(6) to 2.540(6) Å (Table 2).

The two pdc^{3-} ligands in the asymmetric unit of **5** adopt two coordination modes (c and d) as depicted in Scheme 2. In coordination mode c, the pdc^{3-} ligand acts in a μ_8-η^2O,O′,η^2O′,N,η^2N′,O″;,η^1O″,η^1O‴ fashion, chelating the Gd(2e) (Symmetry code: e x, 1.5 − y, −0.5 + z), Cu(1) and Gd(1) centers and bridging the Gd(1d) and Gd(2d) centers, respectively. In mode d, the pdc^{3-} ligand binds in a μ_7-η^1O,η^2O′,N,η^2N′,O″,η^2O″,O‴ fashion, bridging the Gd(2c) center and chelating the Cu(1), Gd(1) and Gd(2) centers, respectively. The sulfate anions are tetradentate (Scheme 2f) and bridge with four Gd(III) ions (Gd(1), Gd(2f), Gd(1f), and Gd(1d), Symmetry code: f x, −1 + y, z).

As shown in Figure 4a, two $Cu^{II}Gd^{III}$ dinuclear units are connected through two μ_2-O(2) bridges to form a dimer, in which the distance between Gd(1) and Gd(1d) center is 4.095

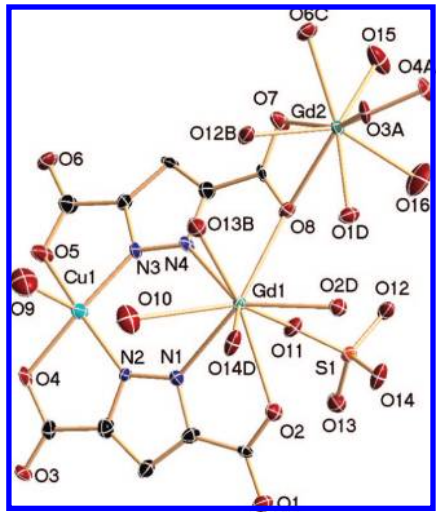

Figure 3. Coordination environments of Gd and Cu atoms in **5** with the thermal ellipsoids drawn at the 50% probability level. All H atoms and noncoordinated water molecules are omitted for clarity. Symmetry codes for the generated atoms see Table 2.

Å. The dimers are further connected together to form an infinite 1D chain (Figure 4b) through three oxygen atoms from the same μ_4-SO_4^{2-} coordinating to the three different Gd(1) centers from two dimers. The eight-membered ring $Gd_2S_2O_4$ is observed. The Gd(2) centers coordinated by O(7) and O(8) from one 1D chain, O(1d), O(3a) and O(4a) from the another chain and the fourth oxygen atom (O(12b)) of the μ_4-SO_4^{2-} lead to the puckered 2D layers (structures c and d in Figure 4), which were interdigitationally arrayed along the crystallographic *a*-direction and linked by O(6) coordinating to the Gd(2) centers to form three-dimensional coordination frameworks (Figure 4e).

Magnetic Properties. The temperature-dependent magnetic susceptibility data of complexes **2** and **4**−**6** have been measured for polycrystalline samples in the temperature range of 1.8−300 K.

Figure 5 shows the temperature dependence of the $\chi_M T$ and χ_M^{-1} curves for complex **2**. At 300 K, the $\chi_M T$ value of **2** is 27.464 cm^3 K mol^{-1}, which is close to the expected value of 28.715 cm^3 K mol^{-1} for one isolated Cu^{II} ion ($S = 1/2$, $g = 2$) and two isolated Dy^{III} ions for the corresponding ground state $^6H_{15/2}$ ($g_J = 4/3$).[1a] There is a continuous decrease in the value of $\chi_M T$ as the temperature is lowered from 300 to 1.8 K, at which point the $\chi_M T$ value is 19.471 cm^3 K mol^{-1}. The linear fit via $\chi_M = C/(T - \theta)$ in the whole temperature range gives the Weiss constant $\theta = -2.50$ K and $C = 27.78$ cm^3 K mol^{-1}. Despite the decrease in $\chi_M T$ values on cooling and the presence of negative θ values for **2**, the nature of the magnetic interaction between Ln(III) and Cu(II) or Ln(III) and Ln(III) ions cannot be unambiguously interpreted as antiferromagnetic because of the strong spin−orbit coupling for lanthanide atoms and the progressive thermal depopulation of the Ln^{III} Stark components.[17]

At 300 K, the $\chi_M T$ value of **4** is 3.244 cm^3 K mol^{-1} (Figure 6). It is much larger than the calculated value of 0.375 cm^3 K mol^{-1} expected for one independent Cu^{II} ion and two independent Eu^{III} ions, assuming that only the ground state $^7F_0$ of the Eu^{III} ion ($4f^6$, $J = 0$, $S = 3$, $L = 3$, $^7F_0$) is thermally populated. The disagreement is ascribed to the presence of thermally populated excited states, as is well-known for Eu^{III} complexes.[18] The $\chi_M T$ value decreases monotonically as the temperature is lowered from 300 to 1.8 K (0.477 cm^3 K mol^{-1} at 1.8 K). The temperature dependence of the $\chi_M T$ can be reproduced by eqs 1, 2, and 3, which takes into account the seven states $^7F_0$, $^7F_1$, $^7F_2$, $^7F_3$, $^7F_4$, $^7F_5$, and $^7F_6$ generated by the interelectronic repulsion and spin−orbit coupling.[18] The best-fit parameter $\lambda = +309$ cm^{-1} (λ is the spin−orbit coupling parameter) was obtained (with an agreement factor $R = \sum[(\chi_M T)_{calcd} - (\chi_M T)_{obsd}]^2/\sum(\chi_M T)_{obsd}^2 = 2.1 \times 10^{-3}$).

$$\chi_M T = 2\chi_{Eu} T + \chi_{Cu} T \quad (1)$$

$$\chi_{Cu} T = Ng^2\beta^2/4k \quad (2)$$

$$\chi_{Eu} T = (N\beta^2/3kx)[24 + (27x/2 - 3/2)e^{-x} + (135x/2 - 5/2)e^{-3x} + (189x - 7/2)e^{-6x} + (405x - 9/2)e^{-10x} + (1485x/2 - 11/2)e^{-15x} + (2457x/2 - 13/2)e^{-21x}]/[1 + 3e^{-x} + 5e^{-3x} + 7e^{-6x} + 9e^{-10x} + 11e^{-15x} + 13e^{-21x}], \text{ with } x = \lambda/kT \quad (3)$$

The $\chi_M T$ value of **5** is 16.001 cm^3 K mol^{-1} at 300 K, which is in agreement with the calculated value (16.135 cm^3 K mol^{-1}) for the presence of two isolated Gd^{III} (ground state $^8S_{7/2}$ and $g_J = 2$)[1a] ions and one $S = 1/2$ Cu^{II}. While the temperature decreases, the $\chi_M T$ value remains roughly constant down to 50 K and then it increases rapidly and reaches maximum of 18.782 cm^3 K mol^{-1} at 1.8 K (Figure 7), indicating predominant ferromagnetic interactions in the complex. The fitting of experimental data with a Curie−Weiss law leads to $C = 16.09$ cm^3 K mol^{-1} and $\theta = 0.24$ K, confirming the presence of ferromagnetic interaction. The magnetization measurements at 1.8 K, done as a function of the field, reveal a clear saturation above 4 T (the inset in Figure 7). The saturation of M at 12.6 $N\mu_B$ is lower than that expected value (15 $N\mu_B$), which are uncoupled or completely ferromagnetically coupled. It suggests that even if ferromagnetic interactions are present, some of the centers are necessarily antiferromagnetically coupled in such a way that the applied magnetic field is not able to align all of the spins parallel to populate the $S = 15/2$ state. Because of the complexity for **5**, its magnetic behavior may be affected by many factors, e.g., the Gd−Gd (4.095 and 4.639 Å for the distances of Gd(1)−Gd(1d) and Gd(1)−Gd(2), respectively), and Cu−Gd (4.474 and 4.208 Å for Cu(1)−Gd(1) and Cu(1)−Gd(2e), respectively) interactions, ligand field effects of the Gd^{3+} ion, etc. We can not find an accurate fit of the magnetic data for this system.

The static magnetic susceptibility of **6** has been measured under a 100 Oe applied magnetic field (Figure 8). At 300 K, the $\chi_M T$ product is equal to 22.773 cm^3 K mol^{-1}, which is slightly smaller than the value (24.015 cm^3 K mol^{-1}) expected for one isolated Cu^{II} ion and two isolated Tb^{III} ions with the corresponding ground state $^7F_6$ ($g_J = 3/2$).[1a] There is a continuous decrease in the values of $\chi_M T$ as the temperature is lowered from 300 to 12 K, at which the $\chi_M T$ product reaches a minimum value of 19.095 cm^3 K mol^{-1}. Upon further lowering the temperature, $\chi_M T$ increases dramatically to reach a value of 20.791 cm^3 K mol^{-1} at 1.8 K. The profile of the $\chi_M T$ vs T curve is strongly suggestive of the occurrence of two competitive phenomena. The decrease of $\chi_M T$ on lowering the temperature in the high-temperature region is most probably governed by the depopulation of the Tb Stark levels, while the increase of $\chi_M T$ at lower temperature may be attributed to a ferromagnetic interaction. Magnetization versus field measurements at 1.8 K

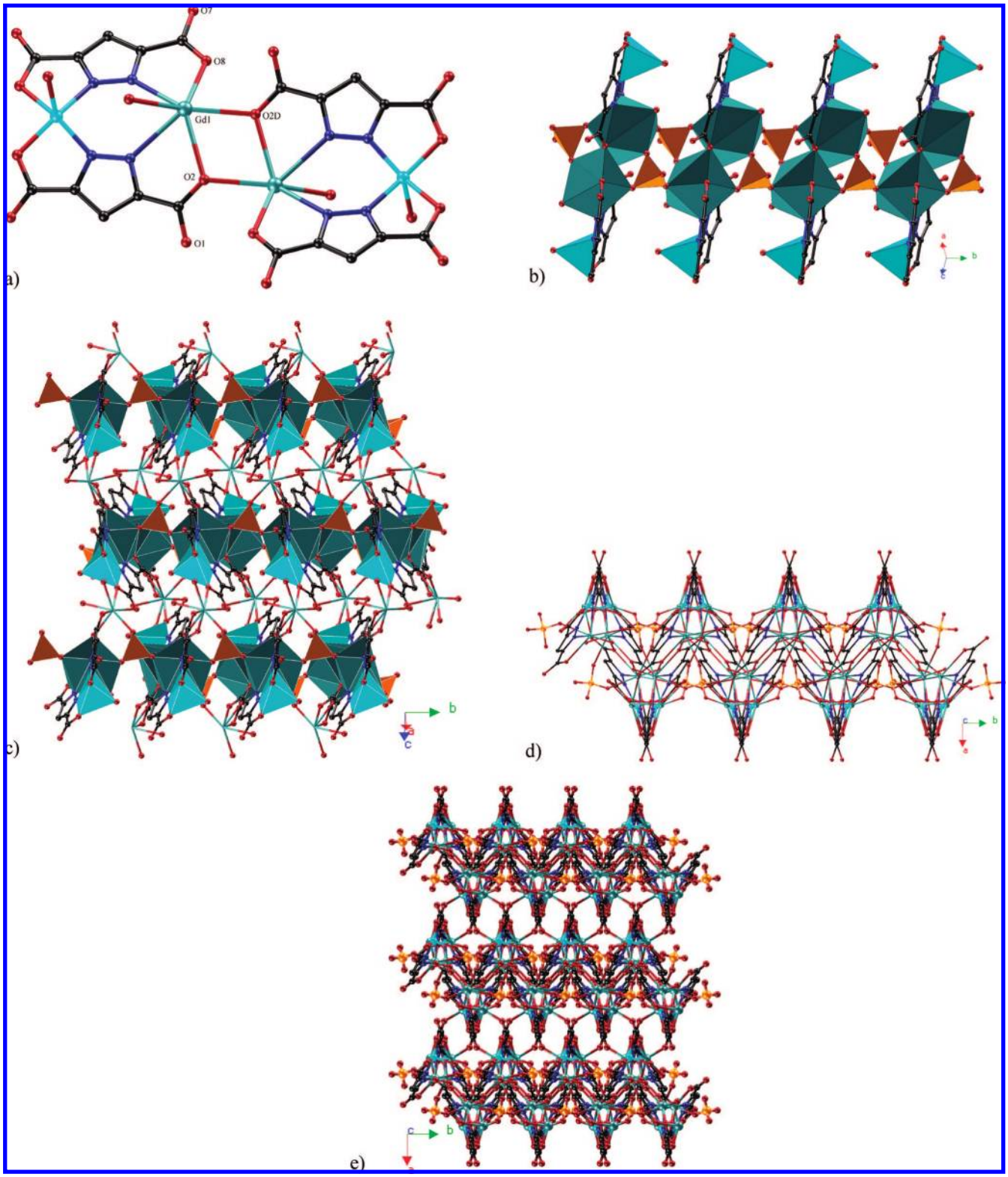

Figure 4. (a) Dimer formed by two $Cu^{II}Gd^{III}$ dinuclear units in **5**. (b) 1D chain formed by SO_4^{2-} anions bridging the dimers. (c, d) 2D network viewed along two different directions. (e) 3D framework of **5** viewed along the *c* axis.

(the inset in Figure 8) shows the saturation value of 9.3 $N\mu_B$ at 7 T, which is much lower than that expected value (19 $N\mu_B$) for two Tb^{III} ($J = 6$, $g_J = 3/2$) ions and one $S = 1/2$ Cu^{II} ion. The results also suggest that ferromagnetic and antiferromagnetic interactions coexist in complex **6**. Similarly, the coupled systems,[19,20] including at least one ion with an orbital momentum, are not amenable to a quantitative analysis.

Conclusion

In summary, seven interesting heterometallic 3d−4f coordination polymers based on pyrazole-bridged $Cu^{II}Ln^{III}$ dinuclear units and sulfate anions are reported. Complexes **1** and **2** are infinite double-stranded tape-like 1D coordination polymers, whereas **3**−**7** display novel 3D framework structures. Although

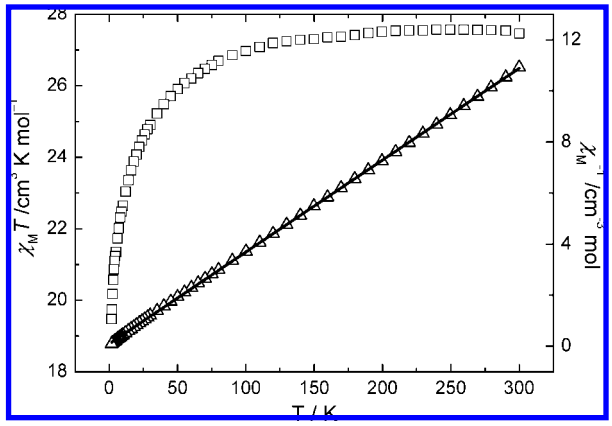

Figure 5. Temperature dependence of the $\chi_M T$ (□) and χ_M^{-1} (△) curves for complex **2**. The solid line represents the best fit obtained with the parameters indicated in the text.

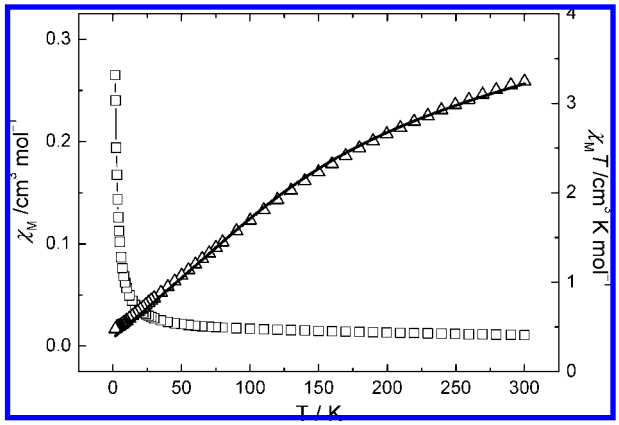

Figure 6. Temperature dependence of the χ_M (□) and $\chi_M T$ (△) curves for complex **4**. The solid line represents the best fit obtained with the parameters indicated in the text.

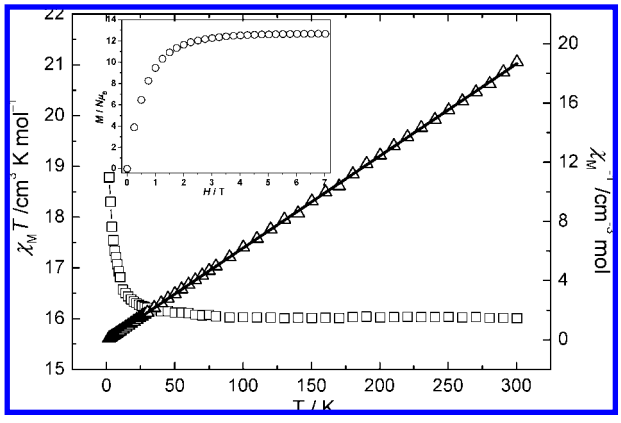

Figure 7. Temperature dependence of the $\chi_M T$ (□) and χ_M^{-1} (△) curves for complex **5**. The solid line represents the best fit obtained with the parameters indicated in the text. Inset: *M* vs *H* plot measured at 1.8 K.

lots of 3d−4f complexes have been reported, examples of heterometallic 3d−4f complexes based on pyrazole-bridged units and sulfate anions are still quite rare so far. Magnetic properties for **2** and **4**−**6** have been studied and ferromagnetic interactions are observed for **5** and **6.** More investigations on pyrazole-bridged heterometallic 3d−4f complexes with interesting structures and magnetic properties and attempts to proposing a theoretical model to account for the magnetizms observed are currently underway in our laboratory.

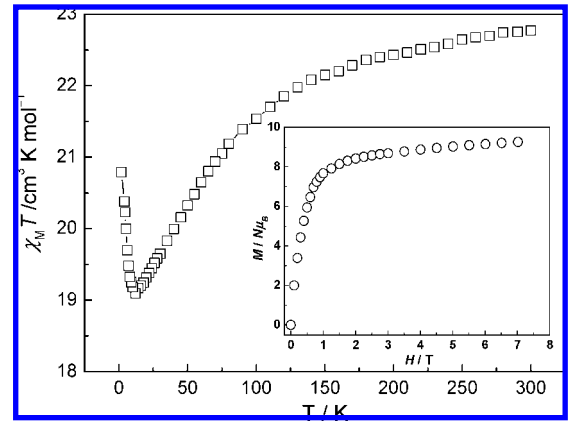

Figure 8. Temperature dependence of the $\chi_M T$ (□) curve for complex **6**. Inset: *M* vs *H* plot measured at 1.8 K.

Acknowledgment. This work was supported by the Major State Basic Research Development Program (2006CB806104 and 2007CB925103), the National Science Fund for Distinguished Young Scholars of China (Grant 20725104), and the National Natural Science Foundation of China (Grant 20721002).

Supporting Information Available: X-ray structure data for **1**−**7** in CIF format and selected bond lengths for **1**, **3**, **4**, **6**, and **7** (Tables S1 and S2) in PDF format. This material is available free of charge via the Internet at http://pubs.acs.org.

References

(1) (a) Bünzli, J. C. G.; Piguet, C. *Chem. Rev.* **2002**, *102*, 1897. (b) Sakamoto, M.; Manseki, K.; Okawa, H. *Coord. Chem. Rev.* **2001**, *379*, 219–221. (c) Ockwig, N. W.; Delgado-Friedrichs, O.; O'Keeffe, M.; Yaghi, O. M. *Acc. Chem. Res.* **2005**, *38*, 176. (d) Benelli, C.; Gatteschi, D. *Chem. Rev.* **2002**, *102*, 2369. (e) Plečnik, C. E.; Liu, S.; Shore, S. G. *Acc. Chem. Res.* **2003**, *36*, 499.

(2) (a) Mereacre, V. M.; Ako, A. M.; Clérac, R.; Wernsdorfer, W.; Filoti, G.; Bartolomé, J.; Anson, C. E.; Powell, A. K. *J. Am. Chem. Soc.* **2007**, *129*, 9248. (b) Ueki, S.; Kobayashi, Y.; Ishida, T.; Nogami, T. *Chem. Commun.* **2005**, 5223. (c) He, F.; Tong, M. L.; Chen, X. M. *Inorg. Chem.* **2005**, *44*, 8285. (d) Cheng, J. W.; Zheng, S. T.; Yang, G. Y. *Inorg. Chem.* **2007**, *46*, 10261. (e) Zhao, B.; Chen, X. Y.; Cheng, P.; Liao, D. Z.; Yan, S. P.; Jiang, Z. H. *J. Am. Chem. Soc.* **2004**, *126*, 15394. (f) Prasad, T. K.; Rajasekharan, M. V.; Costes, J. P. *Angew. Chem., Int. Ed.* **2007**, *46*, 2851.

(3) (a) Andruh, M.; Ramade, I.; Codjovi, E.; Guillou, O.; Kahn, O.; Trombe, J. C. *J. Am. Chem. Soc.* **1993**, *115*, 1822. (b) Andruh, M.; Kahn, O.; Sainto, J.; Dromzee, Y.; Jeannin, S. *Inorg. Chem.* **1993**, *32*, 1623. (c) Benelli, C.; Caneschi, A.; Gatteschi, D.; Guillou, O.; Pardi, L. *Inorg. Chem.* **1990**, *29*, 1750. (d) Georges, R.; Kahn, O.; Guillou, O. *Phys. Rev. B* **1994**, *49*, 3235. (e) Chen, L.; Breeze, S. R.; Rousseau, R. J.; Wang, S.; Thompson, L. K. *Inorg. Chem.* **1995**, *34*, 454. (f) Chen, X. M.; Wu, Y. L.; Tong, Y. X.; Huang, X. Y. *J. Chem. Soc., Dalton Trans.* **1996**, 2443. (g) Sanada, T.; Suzuki, T.; Kaizaki, S. *J. Chem. Soc., Dalton Trans.* **1998**, 959, and references therein. (h) Costes, J. P.; Dahan, F.; Dupuis, A.; Laurent, J. P. *Inorg. Chem.* **1997**, *36*, 3429. (i) He, Z.; He, C.; Gao, E. Q.; Wang, Z. M.; Yang, X. F.; Liao, C. S.; Yan, C. H. *Inorg. Chem.* **2003**, *42*, 2206.

(4) (a) Estrader, M.; Ribas, J.; Tangoulis, V.; Solans, X.; Font-Bardía, M.; Maestro, M.; Diaz, C. *Inorg. Chem.* **2006**, *45*, 8239. (b) Bailey, W. E.; Williams, R. J.; Milligan, W. O. *Acta Crystallogr., Sect. B* **1973**, *29*, 1365. (c) Gheorghe, R.; Cucos, P.; Andruh, M.; Costes, J. P.; Donnadieu, B.; Shova, S. *Chem.—Eur. J.* **2005**, *12*, 187. (d) Boncella, J. M.; Andersen, R. A. *Inorg. Chem.* **1984**, *23*, 432. (e) Figuerola, A.; Ribas, J.; Casanova, D.; Maestro, M.; Alvarez, S.; Diaz, C. *Inorg. Chem.* **2005**, *44*, 6949. (f) Crease, A. E.; Legzdins, P. *J. Chem. Soc., Dalton Trans.* **1973**, 1501. (g) Tilley, T. D.; Andersen,

R. A. *J. Am. Chem. Soc.* **1982**, *104*, 1772. (h) Boncella, J. M.; Andersen, R. A. *Chem. Commun.* **1984**, 809. (i) Plecnik, C. E.; Liu, S.; Chen, X.; Meyers, E. A.; Shore, S. G. *J. Am. Chem. Soc.* **2004**, *126*, 204. (j) Chelebaeva, E.; Larionova, J.; Guari, Y.; Sa Ferreira, R. A.; Carlos, L. D.; Almeida Paz, F. A.; Trifonov, A.; Guerin, C. *Inorg. Chem.* **2008**, *47*, 775. (k) James, C.; Willand, P. S. *J. Am. Chem. Soc.* **1916**, *38*, 1497.

(5) (a) Kawahata, R.; Tsukuda, T.; Yagi, T.; Subhan, M. A.; Nakata, H.; Fuyuhiro, A.; Kaizaki, S. *Chem. Lett.* **2003**, *32*, 1084. (b) Wang, Y.; Song, Y.; Pan, Z. R.; Shen, Y. Z.; Hu, Z.; Guo, Z. J.; Zheng, H. G. *Dalton. Trans* **2008**, 5588.

(6) Viler, R.; Mingos, D. M. P.; White, A. J. P.; Williams, D. J. *Angew. Chem., Int. Ed.* **1998**, *37*, 1258, and refs therein.

(7) (a) Breck, D. W. *Zeolite Molecular Sieves*; Wiley: New York, 1974. (b) Meier, W. M.; Oslen, D. H.; Baerlocher, C. *Atlas of Zeolite Structure Types*; Elsevier: London, 1996.

(8) (a) Cheetham, A. K.; Ferey, G.; Loiseau, T. *Angew. Chem., Int. Ed.* **1999**, *38*, 3268. (b) Rao, C. N. R.; Natarajan, S.; Choudhury, A.; Neeraj, S.; Ayi, A. A. *Acc. Chem. Res.* **2001**, *34*, 80.

(9) (a) Livage, C.; Egger, C.; Ferey, G. *Chem. Mater.* **1999**, *11*, 1546. (b) Reinke, T. M.; Eddaoudi, M.; O'Keeffe, M.; Yaghi, O. M. *Angew. Chem., Int. Ed.* **1999**, *38*, 2590, and refs therein.

(10) (a) Choudhury, A.; Krishnamoorthy, J.; Rao, C. N. R. *Chem.Commun.* **2001**, 2610. (b) Paul, G.; Choudhury, A.; Rao, C. N. R. *J. Chem. Soc., Dalton Trans.* **2002**, 3859.

(11) (a) King, P.; Clérac, R.; Anson, C. E.; Coulon, C.; Powell, A. K. *Inorg. Chem.* **2003**, *42*, 3492. (b) Yang, J. H.; Zheng, S. L.; Yu, X. L.; Chen, X. M. *Cryst. Growth Des.* **2004**, *4*, 831. (c) Pan, L.; Huang, X. Y.; Li, J.; Wu, Y. G.; Zheng, N. W. *Angew. Chem., Int. Ed.* **2000**, *39*, 527.

(12) (a) Pan, L.; Ching, N.; Huang, X. Y.; Li, J. *Chem.—Eur. J.* **2001**, *7*, 4431. (b) Wenkin, M.; Devillers, M.; Tinant, B.; Declercq, J. P. *Inorg. Chim. Acta* **1997**, *258*, 113. (c) Hahn, C. W.; Rasmussen, P. G.; Bayoń, J. C. *Inorg. Chem.* **1992**, *31*, 1963.

(13) *SAINT-Plus*, version 6.02; Bruker Analytical X-ray System: Madison, WI, 1999.

(14) Sheldrick, G. M.; *SADABS: An empirical absorption correction program*; Bruker Analytical X-ray Systems: Madison, WI,1996.

(15) Sheldrick, G. M. *SHELXTL-97*; Universität of Göttingen: Göttingen, Germany, 1997.

(16) Nakamato, K. *Infrared and Raman Spectra of Inorganic and Coordination Compounds*; Wiley-Interscience: New York, 1978.

(17) Kahn, M. L.; Sutter, J. P.; Golhen, S.; Guionneau, P.; Ouahab, L.; Kahn, O.; Chasseau, D. *J. Am. Chem. Soc.* **2000**, *122*, 3413.

(18) (a) Andruh, M.; Bakalbassis, E.; Kahn, O.; Trombe, J. C.; Porcher, P. *Inorg. Chem.* **1993**, *32*, 1616–1622. (b) Kido, T.; Ikuta, Y.; Sunatsuki, Y.; Ogawa, Y.; Matsumoto, N. *Inorg. Chem.* **2003**, *42*, 398–408.

(19) Kahn, M. L.; Mathonière, C.; Kahn, O. *Inorg. Chem.* **1999**, *38*, 3692.

(20) Costes, J. P.; Dahan, F.; Dupuis, A.; Laurent, J. P. *Chem.—Eur. J.* **1998**, *4*, 1616.

CG800848N